arXiv:2609.01896v2 [cs.LG] 27 Oct 2026

OutageDiT: A Foundation Model for Power Outage Forecasting and Scenario Generation

Yunqin Zhu[1] **Feng Qiu**[2] **Yao Xie**[1]
[1]H. Milton Stewart School of Industrial and Systems Engineering,
Georgia Institute of Technology
[2]Argonne National Laboratory
yao.xie@isye.gatech.edu

Abstract

Power-outage planning requires scenarios before an event occurs. These scenarios must represent uncertainty in magnitude, timing, and duration while preserving temporal dependence. However, severe events are rare, and data from any single region contain few examples of extreme outage and restoration patterns. To address this challenge, we introduce OutageDiT, a foundation model for generating seven-day outage trajectories at 15-minute resolution, trained on outage and weather records across the United States. Specifically, a condition encoder processes historical context and known future covariates once per forecast, and a shallow flow-matching decoder reuses the resulting horizon-aligned states to sample complete outage trajectories. This enables point forecasting, uncertainty quantification, and conditional scenario generation within one deep generative model. Across outage forecasting benchmarks, OutageDiT improves forecast accuracy and scenario quality over strong baselines and supports zero-shot transfer to held-out regions. Together, these results position conditional outage scenario generation as a bridge from outage forecasting to operational planning under uncertainty.

1 Introduction

Power-outage response decisions are made before an event's magnitude and duration are fully known. Examples include crew staging and resource allocation, which require probabilistic forecasts of how outage counts may evolve over the planning horizon under uncertainty. Scenario-based planning further requires representative uncertainty realizations [2, 9]. For outage response, these are complete trajectories that preserve temporal dependence and plausible patterns of escalation, peak severity, and restoration. We formulate this task as generating samples from the conditional distribution

$$p\Big(\underbrace{y_{0:T}}_{\text{future outages}} \;\Big|\; \underbrace{h_{-L:0}}_{\text{outage and customer history}}, \underbrace{w_{-L:T}}_{\text{weather covariates}}, \underbrace{a_{-L:T}}_{\text{calendar covariates}}\Big), \tag{1}$$

where L and T denote the numbers of 15-minute time steps in the 14-day history window and seven-day forecast horizon, respectively. Outage trajectories depend on weather as well as local infrastructure, vegetation, and grid vulnerability [3, 7, 8, 19, 21, 24]. Yet severe events are rare within any single region, leaving limited examples of how outages escalate and recover under different conditions. Cross-region pretraining can broaden this coverage by learning shared outage and restoration patterns, while conditioning on local history, weather, and calendar covariates retains regional context. These considerations motivate a foundation model that combines shared patterns with local context to support transfer to regions with little or no local training data.

We develop OutageDiT, a generative foundation model for power outage trajectories, pretrained on outage and weather records across the United States. To incorporate local context, a condition

40th Conference on Neural Information Processing Systems (NeurIPS 2026). Workshop: Second Workshop on MLxOR: Mathematical Foundations and Operational Integration of Machine Learning for Uncertainty-Aware Decision-Making.

encoder maps 14 days of history and covariates available at forecast time to states aligned with the forecast horizon. A shallow decoder based on the Diffusion Transformer (DiT) architecture [13, 14] then reuses these states to capture temporal dependence in future outages. Trained with flow matching [11], the decoder generates trajectories through ODE integration. The resulting trajectories are decoded into nonnegative integer outage counts using an analytic count representation. Across national seven-day forecasting and held-out Michigan benchmarks, OutageDiT improves point and probabilistic forecast accuracy over supervised and fine-tuned foundation-model baselines, better represents temporal dependence and forecast uncertainty in generated scenarios, and transfers directly to a state excluded from training.

2 Method

Count representation. Outage and tracked-customer counts are nonnegative integers with a wide dynamic range (up to 10^7 in our dataset). We represent overall scale and digit-level detail separately, with an analytic inverse that recovers integer counts. Direct decimal encoding, however, is discontinuous at carry boundaries: an increment of one can change several digits. For a count n, let $(d_6, \dots, d_0)$ be its zero-padded decimal digits, with d_0 the units digit. We reflect each lower digit when the next higher digit is odd:

$$r_6 = d_6, \qquad r_j = d_j + (d_{j+1} \bmod 2)(9 - 2d_j), \quad j = 0, \dots, 5.$$

These carry-aware coordinates keep consecutive counts adjacent across carries. We also append a normalized log-magnitude coordinate to provide a monotone summary of scale and determine which decimal positions are valid during decoding. The resulting representation is

$$g(n) = [2\log_{10}(1+n)/7 - 1, (2r_6 - 9)/10, \dots, (2r_0 - 9)/10] \in \mathbb{R}^8. \tag{2}$$

Condition encoder. Recent outages describe the current state, while longer history provides context for how outages respond to weather. We therefore use 14 days of transformed quarter-hour outage and tracked-customer counts with weather and calendar covariates, and represent the most recent day in a separate stream. Four consecutive observations are patched into an hourly token. The condition encoder applies transformer blocks [20] to 336 history tokens, an overlapping 24-token recent count stream, and 168 future tokens formed from weather and calendar variables known over the seven-day horizon. A shared signed hourly time axis aligns these streams through rotary position embeddings (RoPE) [17]. History serves as a read-only key-value bank, allowing recent and future tokens to attend jointly to historical context without updating the history tokens. The final encoder block returns 168 horizon-aligned conditioning states $c = (c_0, \dots, c_{167})$.

Flow decoder. We apply flow matching [11] to generate complete trajectories and model uncertainty jointly across the forecast horizon. To apply this continuous formulation to discrete digit coordinates, we add independent noise $\epsilon_j \sim \mathcal{U}(-0.05, 0.05)$ to each future digit coordinate at every forecast time step without crossing quantization-bin boundaries. Let $\tilde{y}$ denote the trajectory obtained by applying g to each raw count in $y = y_{0:T}$ and adding this noise. With $z \sim \mathcal{N}(0, I)$, we sample $\tau \sim \mathcal{U}(0, 1)$, construct $\tilde{y}_\tau = (1-\tau)\tilde{y} + \tau z$, and train the decoder to predict velocity $z - \tilde{y}$. Since the conditioning states remain fixed while the noisy trajectory changes, a shallow decoder reuses c to predict this velocity. It first patchifies $\tilde{y}_\tau \in \mathbb{R}^{T\times 8}$ into 168 hourly tokens. Each layer then jointly attends to the conditioning states c and noisy future tokens using a single softmax, combining local context with temporal interactions across the forecast horizon. Within each layer, flow time τ modulates the attention and feed-forward residuals through adaptive layer normalization (adaLN) [14]. Finally, the output head maps each hourly token to four quarter-hour velocity predictions. We also use an auxiliary head f_θ to predict $\log(1+y)$ from c at 15-minute resolution, providing direct forecasting supervision to the condition encoder. The full objective is

$$\mathcal{L} = \mathbb{E}\Big[\underbrace{\frac{1}{8T}\|v_\theta(\tilde{y}_\tau, \tau, c) - (z - \tilde{y})\|_F^2}_{\text{flow matching loss}} + \lambda_{\text{aux}} \underbrace{\frac{1}{T}\|f_\theta(c) - \log(1+y)\|_F^2}_{\text{auxiliary loss}}\Big], \tag{3}$$

where λ_{aux} is the auxiliary-loss weight. At inference, the condition encoder runs once, and its layer-wise key-value projections are cached across Monte Carlo samples and ODE solver steps. Sampling starts from $\tilde{y}_1 = z$ and integrates the flow ODE from $\tau = 1$ to $\tau = 0$, updating only the noisy future tokens and their projections. After integration, g^{-1} maps the transformed coordinates back to integer counts. Appendix B provides the complete architecture and optimization details.

Table 1: National seven-day forecasting performance and ablations. All metrics evaluate outage count in $\log_{10}(1+y)$ space. Ablations use the same training budget and evaluation protocol.

(a) Overall performance

	MSE			WQL		
Model	All	Normal	Event	All	Normal	Event
DeepAR	2.356	0.317	4.395	0.664	0.874	0.639
TFT	1.853	0.207	3.499	0.523	0.589	0.515
CSDI	1.445	0.358	2.533	0.489	0.906	0.440
TimesFM 2.5	1.233	0.209	2.257	0.444	0.918	0.388
Chronos-2	1.041	0.190	1.892	0.361	0.550	0.339
OutageDiT	**0.857**	**0.162**	**1.552**	**0.328**	**0.508**	**0.306**

(b) Ablations of OutageDiT

Variant	MSE	WQL	VS
–	**0.857**	**0.328**	**0.151**
w/o history	0.929	0.357	0.163
w/o recent	0.962	0.356	0.156
w/o future	1.346	0.424	0.175
w/o digits	0.903	0.349	0.158
w/o dequant.	0.869	0.331	0.152
w/o aux. loss	0.912	0.345	0.154

3 Experiments

Experimental setup. Training uses U.S. county-level windows outside Michigan ending before 2025. Validation covers January–February 2025 and test covers March–May 2025. Each evaluation split contains 30 normal windows and 30 event windows drawn from ten distinct events. An event must exceed both 800 outages and 4% of tracked customers for at least six hours. Inputs combine historical outage and customer counts, calendar variables, and 84 hourly meteorological covariates derived from NOAA/NCEP High-Resolution Rapid Refresh (HRRR) fields[1]; weather is observed through the forecast horizon. All supervised models use the same county/origin sampling distribution, and validation MSE selects checkpoints. We report MSE and weighted quantile loss (WQL) in $\log_{10}(1+y)$ space; lower values are better. Appendices A, B, C.1, and C.2 provide the data, training, and evaluation details.

National forecasting. Table 1(a) compares OutageDiT with task-trained probabilistic baselines [10, 15, 18] and fine-tuned time-series foundation models [1, 6]. OutageDiT performs best on every split and metric. The advantage holds on normal and event windows, so the aggregate gain is not driven by a single regime. Table 1(b) shows that every conditioning branch contributes. Future conditioning has the largest effect, while the history and recent ablations confirm that both temporal scales remain useful. Digit coordinates and the auxiliary log-count loss provide the largest gains among the remaining components; uniform digit noise yields a smaller but consistent improvement. Figure 1 illustrates complementary high-impact dynamics: the forecast follows restoration and secondary fluctuations in St. Louis, MO, while the Douglas, NE forecast captures event onset one day before the ground-truth peak.

Scenario generation. For models returning complete trajectories, we report the variogram score (VS) and the coverage and width of the central 90% prediction interval. VS is sensitive to temporal dependence; coverage and width assess marginal calibration and sharpness. We also compare with a generative time-series foundation model [12]. Table 2(a) shows that OutageDiT has the lowest VS and highest coverage with interval width comparable to competing methods. Lower coverage on event windows identifies extreme-event calibration as the primary limitation. Figure 2 further shows that digit coordinates bring synthetic one-day trajectories closer to the real joint distribution, consistent with their gains beyond pointwise forecast error.

Geographic transfer. Michigan provides a geographically held-out evaluation: OutageDiT is trained without Michigan data and applied directly to the state. The INFORMS DMDA Workshop Data Challenge reports average 24/48-hour RMSE[2]; SARIMAX is its best-performing forecasting method [22]. The IISE Energy Analytics Challenge reports normal and tail RMSE, nonzero F1, and 95% interval Winkler score[3]. We use the official scores of its winner, the Regime-Switching Time Series Foundation Model (RSFM). Table 2(b) shows that OutageDiT leads every reported transfer metric without Michigan training. The gains span average, normal, and tail errors, nonzero detection, and interval quality, supporting transfer across outage regimes and forecast summaries.

[1] https://emc.ncep.noaa.gov/emc/pages/numerical_forecast_systems/hrrr.php

[2] https://sites.google.com/view/dmdaworkshop2025/data-challenge

[3] https://www.iise.org/Details.aspx?id=54646

Table 2: Scenario quality and zero-shot Michigan transfer. National coverage targets 0.90; Michigan metrics follow the DMDA and IISE challenge protocols.

(a) National seven-day forecasting

Model	VS	Coverage	Width
Sundial	0.207	0.650	1.471
DeepAR	0.354	0.622	1.161
CSDI	0.234	0.607	1.877
OutageDiT	**0.151**	**0.839**	1.483

(b) Michigan competition benchmarks

Model	Avg. RMSE	Normal RMSE	Tail RMSE	Nonzero F1	Winkler
SARIMAX	177.24	59.82	264.28	0.577	–
RSFM	175.59	12.89	286.61	0.649	2615
OutageDiT	**164.21**	**11.82**	**257.58**	**0.715**	**2479**

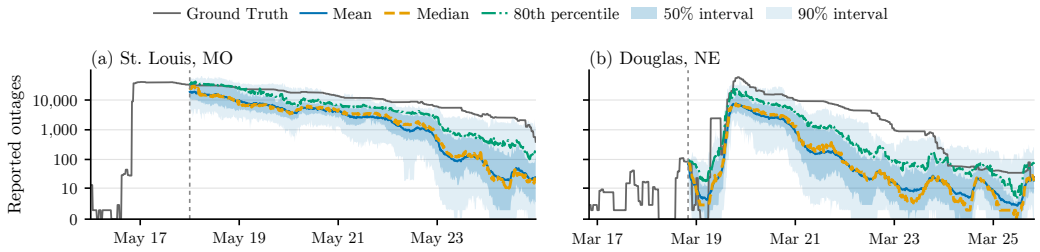

Figure 1: Outage forecasts for (a) restoration in St. Louis, MO and (b) event onset in Douglas, NE. Dashed vertical lines mark forecast origins; bands show central 50% and 90% intervals. Values use the $\log_{10}(1+y)$ scale; dates are in 2025.

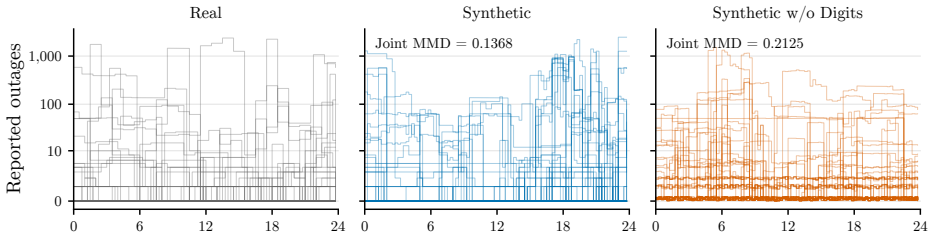

Figure 2: Random one-day outage trajectories. Each panel shows 64 trajectories over a 24-hour forecast horizon. Joint MMD is the empirical RBF-kernel discrepancy over complete trajectories, with bandwidth set to the median pairwise RMS distance among real trajectories.

4 Conclusion

This work introduces OutageDiT, a generative foundation model for conditional seven-day outage trajectories learned from county-level records across the United States. On national benchmarks, OutageDiT improves point and probabilistic forecast accuracy and better preserves scenario-level temporal dependence; ablations attribute these gains to the full conditioning structure and count representation. On Michigan, which is excluded from training, OutageDiT outperforms the reported DMDA and IISE competition baselines across all metrics, demonstrating zero-shot geographic transfer. Extreme-event undercoverage remains the primary limitation. Future work should evaluate these scenarios within crew-staging and resource-allocation decisions, account for weather-forecast error, and extend nominal forecasts to worst-case planning under distribution shift [4, 5, 23].

Acknowledgment

The project is partially supported by the U.S. Department of Energy Advanced Grid Modeling Program under Grant DE-OE 0000875. We thank the NVIDIA Academic Grant Program for providing H100 GPU computing resources through NVIDIA Brev.

References

[1] Abdul Fatir Ansari, Oleksandr Shchur, Jaris Küken, Andreas Auer, Boran Han, Pedro Mercado, Syama Sundar Rangapuram, Huibin Shen, Lorenzo Stella, Xiyuan Zhang, Mononito Goswami, Shubham Kapoor, Danielle C. Maddix, Pablo Guerron, Tony Hu, Junming Yin, Nick Erickson, Prateek Mutalik Desai, Hao Wang, Huzefa Rangwala, George Karypis, Yuyang Wang, and Michael Bohlke-Schneider. Chronos-2: From univariate to universal forecasting. *arXiv preprint arXiv:2510.15821*, 2025.

[2] Dimitris Bertsimas and Nathan Kallus. From predictive to prescriptive analytics. *Management Science*, 66(3):1025–1044, 2020.

[3] Diego Cerrai, David W. Wanik, Md Abul Ehsan Bhuiyan, Xinxuan Zhang, Jaemo Yang, Maria E. B. Frediani, and Emmanouil N. Anagnostou. Predicting storm outages through new representations of weather and vegetation. *IEEE Access*, 7:29639–29654, 2019.

[4] Xiuyuan Cheng, Yao Xie, Linglingzhi Zhu, and Yunqin Zhu. Worst-case generation via minimax optimization in Wasserstein space. *arXiv preprint arXiv:2512.08176*, 2025.

[5] Xiuyuan Cheng, Yunqin Zhu, and Yao Xie. Generative models for decision-making under distributional shift. *arXiv preprint arXiv:2604.04342*, 2026.

[6] Abhimanyu Das, Weihao Kong, Rajat Sen, and Yichen Zhou. A decoder-only foundation model for time-series forecasting. In *Proceedings of the 41st International Conference on Machine Learning*, volume 235 of *Proceedings of Machine Learning Research*, pages 10148–10167. PMLR, 2024.

[7] Seth David Guikema, Roshanak Nateghi, Steven M. Quiring, Andrea Staid, Allison C. Reilly, and Michael Gao. Predicting hurricane power outages to support storm response planning. *IEEE Access*, 2:1364–1373, 2014.

[8] Jichao He, David W. Wanik, Brian M. Hartman, Emmanouil N. Anagnostou, Marina Astitha, and Maria E. B. Frediani. Nonparametric tree-based predictive modeling of storm outages on an electric distribution network. *Risk Analysis*, 37(3):441–458, 2017.

[9] Michal Kaut and Stein W. Wallace. Evaluation of scenario-generation methods for stochastic programming. *Pacific Journal of Optimization*, 3(2):257–271, 2007.

[10] Bryan Lim, Sercan Ö. Arık, Nicolas Loeff, and Tomas Pfister. Temporal Fusion Transformers for interpretable multi-horizon time series forecasting. *International Journal of Forecasting*, 37 (4):1748–1764, 2021.

[11] Yaron Lipman, Ricky T. Q. Chen, Heli Ben-Hamu, Maximilian Nickel, and Matt Le. Flow matching for generative modeling. In *International Conference on Learning Representations*, 2023. URL `https://openreview.net/forum?id=PqvMRDCJT9t`.

[12] Yong Liu, Guo Qin, Zhiyuan Shi, Zhi Chen, Caiyin Yang, Xiangdong Huang, Jianmin Wang, and Mingsheng Long. Sundial: A family of highly capable time series foundation models. In *Proceedings of the 42nd International Conference on Machine Learning*, volume 267 of *Proceedings of Machine Learning Research*, pages 39295–39317. PMLR, 2025.

[13] Nanye Ma, Mark Goldstein, Michael S. Albergo, Nicholas M. Boffi, Eric Vanden-Eijnden, and Saining Xie. SiT: Exploring flow and diffusion-based generative models with scalable interpolant transformers. In *Computer Vision – ECCV 2024*, volume 15135 of *Lecture Notes in Computer Science*, pages 23–40. Springer, 2024.

[14] William Peebles and Saining Xie. Scalable diffusion models with transformers. In *2023 IEEE/CVF International Conference on Computer Vision (ICCV)*, pages 4172–4182, 2023.

[15] David Salinas, Valentin Flunkert, Jan Gasthaus, and Tim Januschowski. DeepAR: Probabilistic forecasting with autoregressive recurrent networks. *International Journal of Forecasting*, 36(3): 1181–1191, 2020.

[16] Michael Scheuerer and Thomas M. Hamill. Variogram-based proper scoring rules for probabilistic forecasts of multivariate quantities. *Monthly Weather Review*, 143(4):1321–1334, 2015.

[17] Jianlin Su, Murtadha Ahmed, Yu Lu, Shengfeng Pan, Wen Bo, and Yunfeng Liu. RoFormer: Enhanced transformer with rotary position embedding. *Neurocomputing*, 568:127063, 2024.

[18] Yusuke Tashiro, Jiaming Song, Yang Song, and Stefano Ermon. CSDI: Conditional score-based diffusion models for probabilistic time series imputation. In *Advances in Neural Information Processing Systems*, volume 34, pages 24804–24816, 2021.

[19] William O. Taylor, Diego Cerrai, David Wanik, Marika Koukoula, and Emmanouil N. Anagnostou. Community power outage prediction modeling for the Eastern United States. *Energy Reports*, 10:4148–4169, 2023.

[20] Ashish Vaswani, Noam Shazeer, Niki Parmar, Jakob Uszkoreit, Llion Jones, Aidan N. Gomez, Łukasz Kaiser, and Illia Polosukhin. Attention is all you need. In *Advances in Neural Information Processing Systems*, volume 30, 2017.

[21] Peter L. Watson, Aaron Spaulding, Marika Koukoula, and Emmanouil Anagnostou. Improved quantitative prediction of power outages caused by extreme weather events. *Weather and Climate Extremes*, 37:100487, 2022.

[22] Haoran Ye, Qiuzhuang Sun, and Yang Yang. SARIMAX-based power outage prediction during extreme weather events. *arXiv preprint arXiv:2511.01017*, 2025.

[23] Linglingzhi Zhu, Yunqin Zhu, and Yao Xie. Distributionally robust optimization via iterative algorithms in continuous probability spaces. In *NeurIPS 2025 ML×OR Workshop*, 2025. URL `https://openreview.net/forum?id=xDRGZLcuN8`.

[24] Shixiang Zhu, Rui Yao, Yao Xie, Feng Qiu, Yueming Qiu, and Xuan Wu. Quantifying grid resilience against extreme weather using large-scale customer power outage data. *INFORMS Journal on Data Science*, 5(2):102–118, 2026.

A Data and Evaluation Protocol

A.1 Data and Inputs

The training dataset contains quarter-hour outage and tracked-customer counts from U.S. counties outside Michigan. Michigan forms a geographically held-out transfer benchmark. Outage records span 2018–2024; complete weather covariates are available from January 2022. Each example contains 14 days of context and a seven-day target, corresponding to 1,344 and 672 quarter-hour observations. The model receives outage and customer-count history, 84 weather variables, and eight calendar variables. Its conditioning path includes observed weather and calendar values over the seven-day forecast horizon. The hourly weather variables are derived from NOAA/NCEP HRRR fields supplied on a county-indexed grid and span temperature, wind, pressure, moisture, cloud, precipitation, convection, and radar diagnostics. Each weather feature is standardized using pre-2025 training data and aligned to its four corresponding quarter-hour observations.

A.2 Training and Evaluation Splits

Training windows follow the natural county-date distribution: each draw first selects a county and then a valid forecast origin in that county. The complete 14-day history stream is retained independently for half of the training examples, while the overlapping 24-hour recent stream is always retained. Weather conditioning is augmented with probabilities 0.80 for full past and future weather, 0.10 for past weather with future weather masked, and 0.10 for all weather masked.

The national validation set contains 30 event and 30 normal windows with origins from January 15 through February 20, 2025; the test set contains the same composition with origins from March 16 through May 23, 2025. The 30 event windows in each split are formed from ten distinct events with three forecast origins per event. An event must exceed both 800 outages and 4% of tracked customers continuously for at least six hours. Normal windows are drawn from counties outside the selected events. Every national score gives equal weight to each forecast case.

B Architecture and Optimization

Four consecutive quarter-hour observations are patchified into one hourly token, yielding 336 history, 24 recent, and 168 future tokens. The condition encoder has four transformer blocks; the flow decoder has two. Both use width 1,024, 16 attention heads with per-head dimension $d_h = 64$, and a feed-forward expansion factor of four. The complete model has 183.46 million trainable parameters. Outage count is the prediction target, and tracked-customer count is a historical covariate.

B.1 Tokenization and Position

We use the outage and customer history h, weather covariates w, and calendar covariates a from Eq. (1). All slices exclude the right endpoint. Token matrices store tokens in columns; LN denotes layer normalization over features, and biases are broadcast across tokens. Layer superscripts distinguish token states from raw time-indexed inputs. For a stream u at 15-minute resolution, locally indexed from zero, each modality m uses the two-layer patch map

$$\mathrm{Patch}_m(u)_i = W_{m,2}\,\mathrm{SiLU}(W_{m,1}\,\mathrm{vec}(u_{4i},\dots,u_{4i+3}) + b_{m,1}) + b_{m,2}. \tag{4}$$

Here vec stacks four observations into a column vector. For count inputs, the transform g in Eq. (2) is applied to each count, and the outage and customer coordinates are concatenated. The three condition streams are

$$\begin{aligned} h^{(0)} &= \mathrm{LN}_h(\mathrm{Patch}_n(g(h_{-L:0})) + \mathrm{Patch}_w(w_{-L:0}) + \mathrm{Patch}_a(a_{-L:0}))\,, \\ r^{(0)} &= \mathrm{LN}_r(\mathrm{Patch}_n(g(h_{-96:0})) + \mathrm{Patch}_a(a_{-96:0}))\,, \\ f^{(0)} &= \mathrm{LN}_f(\mathrm{Patch}_w(w_{0:T}) + \mathrm{Patch}_a(a_{0:T}))\,, \end{aligned} \tag{5}$$

where n, w, a denote count, weather, and calendar modalities. Missing count or weather patches are zeroed before summation. For zero-based hourly index i, the signed positions are $\mathrm{pos}_i^h = i + \frac{1}{2} - 336$, $\mathrm{pos}_i^r = i + \frac{1}{2} - 24$, and $\mathrm{pos}_i^f = i + \frac{1}{2}$. RoPE rotates a query/key vector x at its signed position pos:

$$\begin{bmatrix} \mathrm{RoPE}(x,\mathrm{pos})_{2k} \\ \mathrm{RoPE}(x,\mathrm{pos})_{2k+1} \end{bmatrix} = \begin{bmatrix} \cos(\mathrm{pos}\,\omega_k) & -\sin(\mathrm{pos}\,\omega_k) \\ \sin(\mathrm{pos}\,\omega_k) & \cos(\mathrm{pos}\,\omega_k) \end{bmatrix} \begin{bmatrix} x_{2k} \\ x_{2k+1} \end{bmatrix}. \tag{6}$$

Here $\omega_k = 10{,}000^{-2k/d_h}$ for $k = 0, \ldots, d_h/2 - 1$; RoPE applies these rotations columnwise at the supplied positions. Thus all streams share one time axis, with context before and forecast tokens after the origin.

B.2 Condition Encoder

History tokens remain fixed, $h^{(\ell)} = h^{(0)}$. Nonfinal layers update recent and future tokens; the final layer updates only future tokens. Independent attention and feed-forward norms are indexed by a and f. At layer $\ell = 0, \ldots, 3$, the projections are

$$\begin{aligned} q_s^{(\ell)} &= \mathrm{RoPE}\Big(\mathrm{RMS}_{q,s}^{(\ell)}(W_{q,s}^{(\ell)}\,\mathrm{LN}_{a,s}^{(\ell)}(s^{(\ell)})), \mathrm{pos}^s\Big), \\ k_s^{(\ell)} &= \mathrm{RoPE}\Big(\mathrm{RMS}_{k,s}^{(\ell)}(W_{k,s}^{(\ell)}\,\mathrm{LN}_{a,s}^{(\ell)}(s^{(\ell)})), \mathrm{pos}^s\Big), \\ v_s^{(\ell)} &= W_{v,s}^{(\ell)}\,\mathrm{LN}_{a,s}^{(\ell)}(s^{(\ell)}). \end{aligned} \tag{7}$$

Here $s \in \{h, r, f\}$ labels the stream and pos^s collects its token positions. $q_s^{(\ell)}$ is defined for updated streams, while $k_s^{(\ell)}$ and $v_s^{(\ell)}$ are defined for all three streams. RMS denotes per-head normalization with learned scaling. Each updated stream jointly attends to all three key-value banks:

$$o_s^{(\ell)} = [v_h^{(\ell)}, v_r^{(\ell)}, v_f^{(\ell)}]\,\mathrm{softmax}\left(\frac{[k_h^{(\ell)}, k_r^{(\ell)}, k_f^{(\ell)}]^\top q_s^{(\ell)}}{\sqrt{d_h}} + M_s\right). \tag{8}$$

Here $[\,,\,]$ concatenates token columns, softmax normalizes each column over keys, and M_s masks unavailable history or recent keys. Attention equations are written per head; head outputs are concatenated before the output projection. Each updated stream uses its own pre-normalized residual updates:

$$\bar{s}^{(\ell)} = s^{(\ell)} + W_{o,s}^{(\ell)} o_s^{(\ell)}, \qquad s^{(\ell+1)} = \bar{s}^{(\ell)} + \mathrm{FFN}_s^{(\ell)}(\mathrm{LN}_{f,s}^{(\ell)}(\bar{s}^{(\ell)})), \tag{9}$$

where $\mathrm{FFN}_s^{(\ell)}(x) = W_{2,s}^{(\ell)}[W_{u,s}^{(\ell)} x \odot \mathrm{SiLU}(W_{g,s}^{(\ell)} x)]$, with $\odot$ denoting elementwise multiplication. The encoder returns $c = \mathrm{LN}_{\mathrm{out}}(f^{(4)})$.

B.3 Flow Decoder and adaLN

The noisy trajectory is patched as $x^{(0)} = \mathrm{Patch}_y(\tilde{y}_\tau)$. A Fourier flow-time embedding and multilayer perceptron (MLP) produce

$$e_\tau = \mathrm{MLP}([\sin(\tau\nu); \cos(\tau\nu)]), \qquad (\beta_a, \gamma_a, \alpha_a, \beta_f, \gamma_f, \alpha_f) = W_{\mathrm{mod}}\,\mathrm{SiLU}(e_\tau), \tag{10}$$

where ν is a fixed frequency vector. The parameters β, γ, α provide feature-wise shift, scale, and residual gate, with a, f indexing attention and feed-forward branches. Each layer has its own modulation map (indices omitted); plain LN has no learned affine parameters. For layer $\ell = 0, 1$, let

$$\widehat{x}^{(\ell)} = \mathrm{LN}(x^{(\ell)}) \odot (1 + \gamma_a) + \beta_a. \tag{11}$$

The projections $q_x^{(\ell)}, k_x^{(\ell)}, v_x^{(\ell)}$ follow Eq. (7), with $s = x$ and $\widehat{x}^{(\ell)}$ replacing $\mathrm{LN}_{a,s}^{(\ell)}(s^{(\ell)})$. Both future and condition tokens use pos^f. The projected condition $c_d = W_c c + b_c$ supplies per-layer cached keys and values $(k_c^{(\ell)}, v_c^{(\ell)}) = \mathrm{KV}^{(\ell)}(\mathrm{LN}_c^{(\ell)}(c_d))$. Here $\mathrm{KV}^{(\ell)}$ includes the key/value projections, followed by $\mathrm{RMS}_{k,c}^{(\ell)}$ and RoPE on the keys. Decoder attention is one joint softmax,

$$o_x^{(\ell)} = [v_c^{(\ell)}, v_x^{(\ell)}]\,\mathrm{softmax}\left(\frac{[k_c^{(\ell)}, k_x^{(\ell)}]^\top q_x^{(\ell)}}{\sqrt{d_h}}\right), \tag{12}$$

followed by gated residual updates

$$\begin{aligned} \bar{x}^{(\ell)} &= x^{(\ell)} + \alpha_a \odot \big(W_{o,x}^{(\ell)} o_x^{(\ell)}\big), \\ x^{(\ell+1)} &= \bar{x}^{(\ell)} + \alpha_f \odot \mathrm{FFN}_x^{(\ell)}\Big(\mathrm{LN}(\bar{x}^{(\ell)}) \odot (1 + \gamma_f) + \beta_f\Big). \end{aligned} \tag{13}$$

The output head uses its own flow-time-conditioned shift and scale,

$$v_\theta(\tilde{y}_\tau, \tau, c) = \mathrm{Unpatch}\Big(W_v[\mathrm{LN}(x^{(2)}) \odot (1 + \gamma_o) + \beta_o]\Big), \tag{14}$$

where $(\beta_o, \gamma_o) = W_o\,\mathrm{SiLU}(e_\tau)$ and Unpatch reshapes each hourly output into four quarter-hour velocities. The condition key-value cache is fixed across ODE solver steps and Monte Carlo samples; only the future-token projections are recomputed.

B.4 Model and Training Configuration

Table 3: Configuration of the reported OutageDiT model. SD: standard deviation; LR: learning rate; EMA: exponential moving average; MC: Monte Carlo.

Setting	Value	Setting	Value
Parameters	183.46M	Tokens (history / recent / future)	336 / 24 / 168
Encoder / decoder blocks	4 / 2	Width / heads	1,024 / 16
Patch size	4	Feed-forward expansion	4×
RoPE base	10^4	Flow-time scale	10^3
adaLN initialization SD	10^{-3}	Auxiliary-loss weight	10^{-3}
Optimizer	Muon + AdamW	Batch / maximum updates	512 / 25,000
LR / warmup / schedule	10^{-4} / 500 / constant	EMA decay / start	0.999 / 1,000
ODE solver / steps	Euler / 20	MC samples	64
Sampling noise	Scrambled Sobol Gaussian	Checkpoint selection	Validation MSE

During analytic decoding, the magnitude coordinate selects valid decimal positions before inversion of the reflected digits. The auxiliary head f_θ is linear and uses $\lambda_{\text{aux}} = 10^{-3}$ in Eq. (3).

All linear maps are initialized with Xavier-uniform weights and zero biases, except the flow-time MLP, whose linear weights use a normal distribution with standard deviation 0.02. Adaptive-normalization modulation weights in the flow decoder use a zero-mean Gaussian with standard deviation 10^{-3}. The final modulation and output projection are initialized to zero.

We optimize two-dimensional hidden matrices in the transformer blocks with Muon and all remaining parameters with AdamW. Training uses bfloat16 mixed precision. An exponential moving average begins at update 1,000. Validation is run every 500 updates. Probabilistic and Michigan metrics are evaluated after model selection.

B.5 Baseline Configuration

The supervised baselines use the same county/origin sampler and available covariates. DeepAR is a two-layer autoregressive LSTM with a Student-t likelihood; TFT uses one LSTM layer, hidden size 64, four attention heads, and nine quantiles from 0.1 to 0.9. CSDI treats the future outage window as missing and retains four quarter-hour phases in each hourly patch. TimesFM 2.5[4] is jointly fine-tuned with one shared linear covariate head, and Chronos-2 is fully fine-tuned through its released interface. All checkpoints are selected on validation data and fixed before test and Michigan evaluation. All supervised baselines use AdamW with 500 warmup updates followed by a constant learning rate. Chronos-2 uses the released interface's default learning rate of 10^{-6}. For the remaining baselines, we select the learning rate from $\{10^{-4}, 10^{-3}\}$ using validation MSE.

C Metric Definitions

C.1 National Metrics

Final generative evaluation uses $M = 64$ trajectories generated from scrambled Sobol Gaussian noise with 20 Euler steps. Let N be the number of cases in the evaluated subset, $T = 672$, and $s(y) = \log_{10}(1 + y)$. For sample models, $\widehat{s}_{n,t} = M^{-1} \sum_m s(y_{n,t}^{(m)})$; quantile-only models use their median. The case-equal mean squared error is

$$\text{MSE} = \frac{1}{NT} \sum_{n=1}^{N} \sum_{t=0}^{T-1} \left[\widehat{s}_{n,t} - s(y_{n,t})\right]^2 . \tag{15}$$

For $\mathcal{Q} = \{0.1, 0.2, \ldots, 0.9\}$, let $\widehat{s}_{n,t}^{(q)}$ denote the predictive q-quantile of $s(y_{n,t})$. Weighted quantile loss is

$$\text{WQL} = \frac{2 \sum_n \sum_t \sum_{q \in \mathcal{Q}} \rho_q\Big(s(y_{n,t}) - \widehat{s}_{n,t}^{(q)}\Big)}{|\mathcal{Q}| \sum_n \sum_t |s(y_{n,t})|}, \quad \rho_q(e) = \max\{qe, (q-1)e\}. \tag{16}$$

[4] `https://huggingface.co/google/timesfm-2.5-200m-pytorch`

Sample-based models use empirical quantiles of the same 64 trajectories.

For interval level $1-\alpha$, let $l_{n,t}$ and $u_{n,t}$ be the empirical $\alpha/2$ and $1-\alpha/2$ quantiles in transformed space. We report

$$\mathrm{Coverage}_{1-\alpha} = \frac{1}{NT}\sum_{n=1}^{N}\sum_{t=0}^{T-1}\mathbf{1}\{l_{n,t} \le s(y_{n,t}) \le u_{n,t}\}, \tag{17}$$

$$\mathrm{Width}_{1-\alpha} = \frac{1}{NT}\sum_{n=1}^{N}\sum_{t=0}^{T-1}(u_{n,t} - l_{n,t}), \tag{18}$$

with $\alpha = 0.10$ in Table 2(a).

Temporal dependence is measured by the variogram score of order 0.5 [16]:

$$\mathrm{VS}^{(n)} = \frac{2}{T(T-1)}\sum_{t<t'}\Big(|s(y_{n,t}) - s(y_{n,t'})|^{1/2} - \frac{1}{M}\sum_{m=1}^{M}|s(y_{n,t}^{(m)}) - s(y_{n,t'}^{(m)})|^{1/2}\Big)^2, \tag{19}$$

and the reported value is $N^{-1}\sum_{n=1}^{N}\mathrm{VS}^{(n)}$.

C.2 Michigan Metrics

The transfer evaluation uses all held-out Michigan counties, indexed by $i = 1, \ldots, C$, and the official 48-hour target. Michigan metrics are computed in the original count space, whereas the national metrics above use $s(y)$. OutageDiT uses weather over the 48-hour forecast horizon, following our national evaluation protocol, while the reported competition entries follow their original challenge input protocols. Let $\widehat{y}_{i,t}$ denote the county-hour point forecast, with t indexing hours. The county-macro 24-hour RMSE is

$$\mathrm{RMSE}_{24} = \frac{1}{C}\sum_{i=1}^{C}\sqrt{\frac{1}{24}\sum_{t=0}^{23}(\widehat{y}_{i,t} - y_{i,t})^2}. \tag{20}$$

Define RMSE_{48} analogously over 48 hours. The DMDA average RMSE is

$$\mathrm{RMSE}_{\mathrm{avg}} = \tfrac{1}{2}\left(\mathrm{RMSE}_{24} + \mathrm{RMSE}_{48}\right). \tag{21}$$

For the IISE challenge metrics, κ_i is county i's 95th-percentile training outage count. Let $\mathcal{A}_i^{\mathrm{normal}} = \{t : y_{i,t} < \kappa_i\}$ and $\mathcal{A}_i^{\mathrm{tail}} = \{t : y_{i,t} \ge \kappa_i\}$ over the 48-hour target. Then

$$\mathrm{RMSE}_r = \frac{1}{C}\sum_{i=1}^{C}\sqrt{\frac{1}{\max\{1, |\mathcal{A}_i^r|\}}\sum_{t\in\mathcal{A}_i^r}(\widehat{y}_{i,t} - y_{i,t})^2}, \quad r \in \{\mathrm{normal}, \mathrm{tail}\}. \tag{22}$$

Nonzero F1 labels a county-hour positive when its count is at least one. After pooling all county-hours,

$$F_1 = \frac{2\mathrm{TP}}{2\mathrm{TP} + \mathrm{FP} + \mathrm{FN}}. \tag{23}$$

Here TP, FP, and FN count true positives, false positives, and false negatives, respectively.

The 95% interval uses the empirical 2.5th and 97.5th percentiles of the 64 generated trajectories. For lower and upper bounds (l, u), its Winkler score is

$$W_{0.05}(y, l, u) = (u - l) + 40(l - y)\mathbf{1}\{y < l\} + 40(y - u)\mathbf{1}\{y > u\}, \tag{24}$$

averaged over all $C \times 48$ county-hours.

For Table 2(b), the point summary for each metric is selected on validation data and fixed before Michigan evaluation: the median for normal RMSE, and the 80th percentile for average RMSE, tail RMSE, and nonzero F1. Winkler uses the sample-based 95% interval.

D Additional Forecast Examples

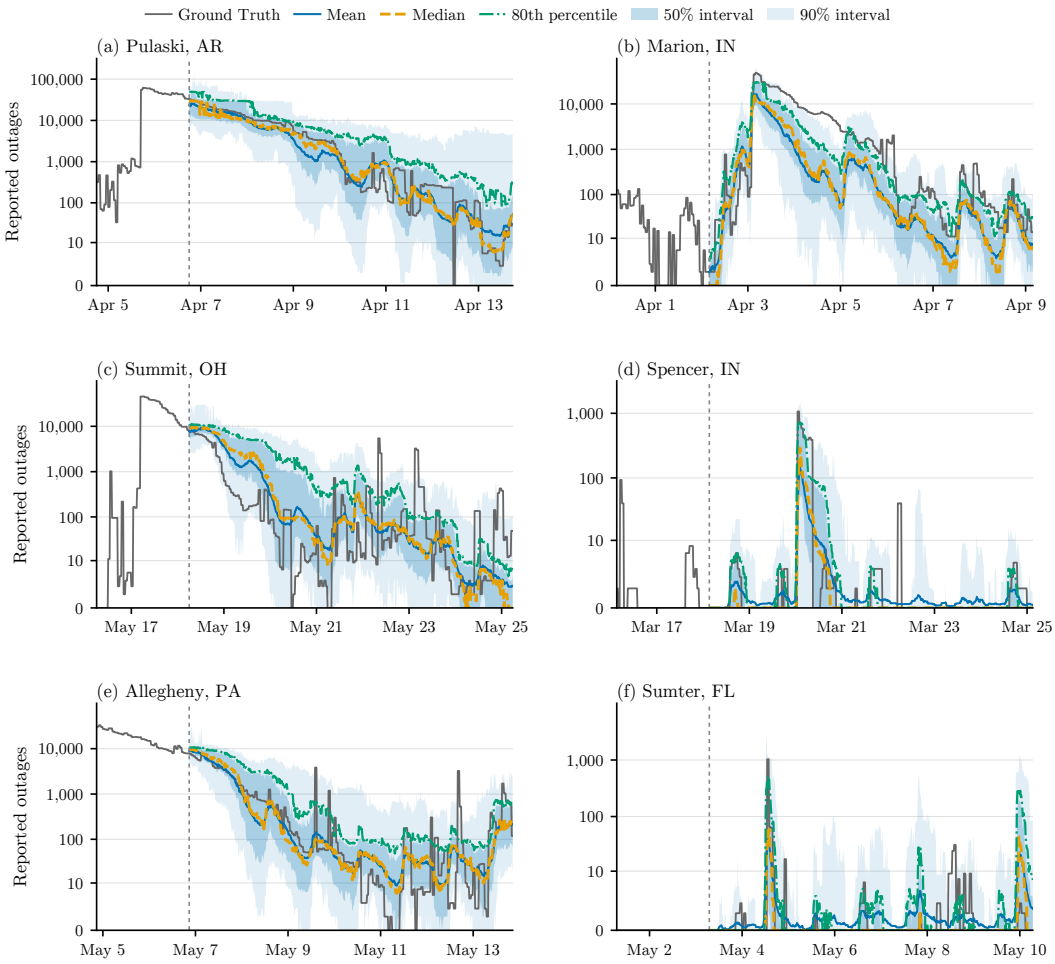

Figure 3: Additional recovery (left) and onset (right) forecasts. All dates are in 2025.